PSNR based optimization applied to Maximum Likelihood Expectation Maximization for image reconstruction on a Multi-core system

[*]MRs.A.Bharathi Lakshmi, [#]Dr.D.Christopher Durairaj, [@]Mrs.T.Veiluvanthal

Asst. Prof.& Head of IT, VVVC, Virudhunagar , Associate Professor in CS. VHNSNC, Virudhunagar, Asst. Prof. of IT, VVVC, Virudhunagar.

ABSTRACT

Image Reconstruction Techniques (IRTs) has been conceded using various reconstruction algorithms. Compared to Analytical image reconstruction method, Statistical image reconstruction methods best suites to reconstruct a high quality image. However, time complexity is involved in it. To overcome the time complexity Maximum Likelihood Expectation Maximization (MLEM) algorithm is parallelized in a multi-core environment. This work concentrates on parallelizing MLEM to reconstruct an image on a shared memory environment in order to reduce the reconstructing time. An attempt is made to optimize the Iteration to reconstruct an image. The performance analyses are employed to know the timeliness, speedup and efficiency for both Sequential and Parallel MLEM. Phantom data set of various sizes under different number of projections is used in our present study. The research shows that the multi-core environment provides the source of high computational power leading to reconstruct an image promptly.

Keywords: *Image Processing, Image Reconstruction, Iterative Image Reconstruction, Maximum Likelihood Expectation Maximization, Parallel Processing, Open MP*

Introduction

Converting an analog image into digital form by carrying out some operations with the image is known as Digital Image Processing (DIP). Mathematical process applied on a Projection data obtained by sweeping magnetic fields at different angles over an object producing an image is generally referred to as Image reconstruction. The image reconstruction is one of the significant applications of the projection technique which is mainly interrelated to the medical image processing technique [1]. DIP has a dynamic abode in the Medical field. Some of the known applications of DIP in the area of medicine are PET scan, Gamma-ray imaging, Radio Waves, Medical CT, X-ray imaging, and Ultra Violet (UV) imaging.

The medical imaging methods are processed using some imaging modalities such as Magnetic Resonance Imaging (MRI), Computed Tomography (CT), Positron Emission Tomography (PET) and etc. It can be processed with the help of Computer Aided Diagnosis (CAD) in order to analyze the inner parts of the human body. Image reconstruction is central to these medical imaging applications. The reconstruction algorithm reduces the noise and reconstructs the images with high quality. Image reconstruction is a kind of mathematical representation in which it generates an image from projections and it collects the data from various angle around Region of Interest (ROI). ROI refers to the phantom or an organ of animal or human. The reconstruction has the basic concepts of image eminence and radiation problem. Improving the quality of the images is a main concept of the reconstruction processbecause the blurred image cannot produce the exact solution to the physician.

Image reconstruction is one type of method to arrange the pixel values in the exact position of the image without noise. Image reconstruction has been carried out using different types of reconstruction algorithms [2, 3]. Reconstruction methods utilize projection data as input and generate the estimate that resembles the internal structure as output [4, 5]. The projections are obtained using the detector ring around the object and are reconstructed using various reconstruction algorithm [2]. Data sets with 36 projections measured from $0^0$to 180^0 around the phantom object were considered in the present study. The same dataset was used for testing the capability of the algorithms from a restricted number of projections, by skipping projections at uniform angular distribution. The research study presented here explores various reconstruction techniques using these types of projections.

Image reconstruction algorithms can be classified into Analytical and Iterative methods. The Analytical image reconstruction methods uses noise free images.

Back Projection (BP) and Filtered Back Projection (FBP) reconstructs the image based on direct inversion of the radon transform derived using a continous line integral. FBP introduces streak artifacts due to limited number of photon emission. Regardless of this disadvantage, FBP is expansively used in nuclear medicine because of its fast reconstruction time [2]. FBP rconstructs the image based on direct inversion of the radon transform derived using a continous line integral. FBP introduces streak artifacts due to limited number of photon emission. Regardless of this disadvantage, FBP is expansively used in nuclear medicine because of its fast reconstruction time [6]. For noisy projection data as well as for a limited number of projections, the FBP method of image reconstruction shows very poor performance. Hence currently there is considerable interest to evaluate the use of other reconstruction methods for medical imaging techniques [5]. FBP algorithm produces high-quality images with excellent computational efficiency. However, FBP produces low Signal-to-Noise Ratio (SNR) images when a limited number of projections is used [7]. An Iterative method using a non-linear fit to the projection data has shown to give ripple free images [8]. Iterative Methods are based on optimization strategies incorporating specific constraints about the object and the reconstruction process. The iterative method can be classified into Algebraic and Statistical methods. Some of the accepted Algebraic iterative algorithms are Additive Algebraic Reconstruction Technique (AART) and Multiplicative Algebraic Techniques (MART) [7].

Statistical image reconstruction plays a vital role in the medical field. Statistical methods for image reconstruction can provide spatial resolution and noise properties over conventional Filtered Back Projection (FBP) methods [5]. However such methods suffer from time complexity. The statistical method is considered as an iterative method in that it can be divided into weighted and likelihood [9]. As the repetition steps are high in the statistical method, it does not suit for all approaches. Iterative process includes the different methods for statistical reconstruction technique in the form of poisson process. The poisson statistical model supports the maximum posteriori work, maximum likelihood, context-based Bayesian framework. Expectation Maximization (EM) is one type of statistical method for image reconstruction process. EM Algorithm is an iterative algorithm that is often used for estimating parameters of Gaussian Mixture Model [10]. The statistical model supports the iterative process to identify maximum posteriori parameters. MLEM is a prevalent technique applied to reconstruct the emission intensity. The popularity of MLEM is due to the high degree of accuracy in the compensation of non-uniform attenuation. However, it occupies high computational time. The core part is to improve the MLEM algorithm computation complexity by accomplishing a innovative technique to reconstruct the image with reduced time complexity attaining better efficiency in speed. This is attained by three step process such as Optimising number of iterations, reconstrucing the image with limited number of projections both sequetial and parallel environment.In present study

Methodologies

For the reconstruction process the emitted and the detected photons are assumed to be Poisson random variables. Hence, in the statistical reconstruction algorithms, the emission data is modeled first and then an estimate of the source distribution is derived. Accordingly, the statistical principle is to govern the source distribution of the emission data by means of the Expectation-Maximization algorithm.

Expectation conditional maximization (ECM) surrogates every M step with an arrangement of conditional maximization (CM) paces in which every single parameter $\boldsymbol{\theta_i}$exhausts the possibilities exclusively, provisionally proceeding on the other parameters remaining fixed.

In the ML-EM algorithm, the projection data collected plays an important role. In a SPECT scanner, the size of the projection data depends on both the quantity of detectors and the corresponding quantity of angles [11]. If the medical imaging modalities has b number of detectors and we measure at a angles, then the total number of counts is the projection data is $\boldsymbol{J = a * b}$. For ease of calculations, this vector is generally epitomized by way of a column vector. In PET, there is a ring of detectors around the patient which measures the annihilation event. An event is recorded only if the two events occur within a time window. If the detector ring has N detectors, the number of counts in projection data is given by $\boldsymbol{J = N(N-1)/2.}$ The image matrix could be accessed as a column vector I with $I = nx * ny$ elements. Practitioner agreed that such emissions follow a Poisson model. Therefore, the unknown total number of emission events in the $\boldsymbol{ith}$ pixel, $\hat{\boldsymbol{x}}(\boldsymbol{i})$ represents a Poisson random variable, with mean$\bar{\boldsymbol{x}}(\boldsymbol{i})$. The system matrix characterizes the probability distribution of the projection data. Hence elements of the system matrix $\boldsymbol{p(i,j)}$ embodies the likelihood of emission i to be detected by detector j. The system matrix will be elucidated in detail in well ahead sections. It is conceivable to estimate the probable value of the projection data depending on the system matrix using the Eq. 1.

$$\hat{n}(j) = E\big(n(i)\big) = \sum_{i=1}^{I} x(i).p(i,j) \qquad (1)$$

The probability of the entire projection dataset is the product of distinct counts, so the likelihood function is given in Eq. 2.

$$L(x) = P\left(\frac{n}{x}\right) = \prod_{j=1}^{j} \frac{e^{-\hat{n}(j)}\hat{n}\,^{n(j)}}{n(j)!} \qquad (2)$$

To simplify the beyond computation we take the log on both sides and its derivation is shown in Eq. 3, Eq. 4 and Eq. 5.

$$l(x) = \log(L(x)) \qquad (3)$$

$$l(x) = \sum_{j=1}^{j}(log\big(e^{-\hat{n}(j)}\big) + log\big(\hat{n}(j)^{n(j)}\big) - log(n(j)!) \qquad (4)$$

$$l(x) = \sum_{j=1}^{j} -(\hat{n})(j) + n(j)log\big(\hat{n}(j)\big) - log(n(j)!) \qquad (5)$$

Replacing Eq. 1 we work out at the log-likelihood function obtains Eq. 6.

$$l(x) = -\sum_{j=1}^{j}\sum_{i=1}^{I} x(i)p(i,j) + \sum_{j=1}^{j} n(j)log\left(\sum_{i=1}^{I} x(i)p(i,j)\right) - \sum_{j=1}^{j} \log(n(j)!) \qquad (6)$$

It can be shown using the first and second derivatives of the log-likelihood function resultant that the applied matrix of second derivatives is negative semi definite and that l(x) is concave. As a result, sufficient conditions for a vector $\hat{x}$ to yield a maximum of l(x) are the Kuhn-Tucker conditions as specified in Eq. 7 and Eq. 8.

$$\left(x(i)\frac{\partial l(x)}{\partial x(i)}\right) = -\hat{x}(i) + -\sum_{j=1}^{j} \frac{n(j)x(i)\widehat{p(i,j)}}{\sum_{j'=1}^{I}\hat{x}(i')p(i',j)} \qquad (7)$$

And

$$\left(\left(x(i)\frac{\partial l(x)}{\partial x(i)}\right)_{\hat{x}}\right) = \leq 0 \ldots\ldots if\ \hat{x}(i) = 0 \qquad (8)$$

The algorithm requires an initial estimate x^0, and using the maximization condition iteratively improves the estimate. Eq. 9 is the main formula for ML-EM algorithm derived by solving the above maximization condition for $\hat{\boldsymbol{x}}(\boldsymbol{i})$

$$x^{n+1}(i) = x^n(i)\sum_{j=1}^{j} \frac{n(j)p(i,j)}{x^n(x')p(i',j)} \qquad (9)$$

This can be written as

$$x^{n+1}(i) = x^n(i)\Delta x^n(i) \qquad (10)$$

Hence from the Eq. 10. the sum is really a multiplicative coefficient that corrects the image at every step. As per the amount of iterations increase, the $\Delta x^n(i)$term gets nearer and nearer to 1.

The accuracy of image reconstruction depends on the reduction of errors, which lies on number of iterations. However, if the number of iterations is too high, due to the Poisson nature of the data, the image may look a little noisy.

The system matrix is the most important part of the ML-EM algorithm. It contains the information of the geometry of the imaging system being used and the mapping from the image space to the data space. The accurate system matrix improve the quality of the reconstructed image. Errors are inevitable in the system matrix, it is important to understand their effect proceeding iterative image rebuilding towards determining the necessary correctness intended for system matrices.

System matrix refers to the association among projection and image space. This association could exist such as the Eq. 11.

$$\boldsymbol{p_j} = \sum_i \boldsymbol{a_{ij}}\boldsymbol{f_i} \qquad (11)$$

Where $\boldsymbol{p_j}$ refers to the true value of the corresponding projection data in lieu of a line of response (LOR) obvious through the detector pair$\boldsymbol{j}$. $\boldsymbol{f_i}$ Stands the importance of image by the side of voxel $\boldsymbol{i}$. $\boldsymbol{a_{ij}}$ is the probability of noticing a concurrence incident instigating commencing voxel $\boldsymbol{i}$ at detector pair $\boldsymbol{j}$. We express A by means of the matrix of $\boldsymbol{a_{ij}}$. Therefore $\boldsymbol{A}$ exemplifies system matrix that could be alienated keen on a number of factored matrices. It could be conveyed as in Eq. 12.

$$\boldsymbol{A} = \boldsymbol{A_{sens}}\boldsymbol{A_{atten}}\boldsymbol{A_{blur}}\boldsymbol{A_{geom}}\boldsymbol{A_{positron}} \qquad (12)$$

$\boldsymbol{A_{positron}}$ that means of positron range factor is moderately lesser and could be unnoticed for F. $\boldsymbol{A_{atten}}$stands for attenuation factor could be fetched through additional CT scan and the detector sensitivity factor. $\boldsymbol{A_{sens}}$ could be attained by way of evaluating a identical cylindrical source. The residual factors are geometrical factor $\boldsymbol{A_{geom}}$ and the blurring factor $\boldsymbol{A_{blur}}$. Through analytical methods the $\boldsymbol{A_{geom}}$ and $\boldsymbol{A_{blur}}$ can be calculated. But calculating $\boldsymbol{A_{blur}}$ is a complex task that influence much deviation in image reconstruction. The physical impacts like crystal penetration and photon non-colinearity increase the blurring issue.

The concept of image rebuilding as of projections could be deliberated by means of system of linear equations Eq. 13 of the procedure:

$$\boldsymbol{Ax} \approx \boldsymbol{B} \qquad (13)$$

The elements of matrix A is subjected to the number of projection and the denoted projection angle. The intensity of the image is characterized by the column matrix x and projections is referred by the column matrix b.

For a certain angle, we take up that the number of projections ranges from 1 to m. For $\boldsymbol{k}$ different angles,

b has $\boldsymbol{M = mxk}$ elements, $\boldsymbol{x}$ has $\boldsymbol{N}$ elements, and $\boldsymbol{A}$ is an $\boldsymbol{MxN}$ rectangular matrix.

$$A=\begin{bmatrix} a_{11} & a_{12} & \dots & a_{1N} \\ a_{21} & a_{22} & \dots & a_{2N} \\ \dots & \dots & \dots & \dots. \\ a_{M1} & a_{M2} & \dots & a_{MN} \end{bmatrix}, b = [b_1 \quad b_2 \quad \dots \quad b_M]^T,$$

$x= [x_1 \quad x_2 \quad \dots \quad x_N]^T,$

Fig. 1 illustrates the data acquirement process during scanning. The entire image is signified in each row and the entire projection data is represented by one column of the system matrix. Thus, a fixed row in the system matrix corresponds to a particular detector at a particular angle.

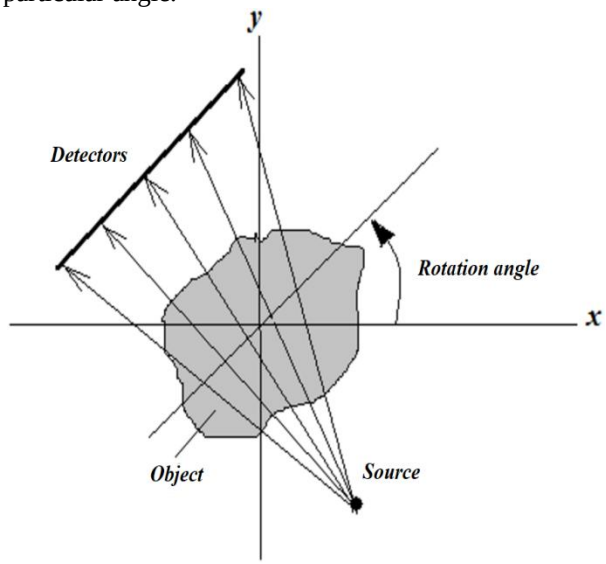

Fig. 4.1: The data acquirement process during scanning.

Since this matrix contains the probability of an emission at an exact point showing up at an exact detector at an exact angle, many elements within this matrix are zeros. Very few pixels in this matrix will have non-zero terms. This makes the system matrix very sparse.

When applying iterative Maximum Likelihood approaches to restoration or reconstruction of blurred and noisy images. Ideally, one would carry on repeating till the Kuhn-Tucker conditions are satisfied. Furthermost of such kind of iterative procedures primarily converge rapidly nevertheless making very gentle convergence in the far ahead repetitions. In emission tomography, there might be need for more than a hundred ML repetitions may possibly be necessary intended for the Kuhn-Tucker Conditions to be gratified near a number of digits. The image reconstruction will be worsening even after some iteration of image reconstructions because of excessive non-smooth advent. From simulations, we can learn that the squared error between the estimate and true image instigates to prolife in this certain point. The supreme striking and accurate refurbishments and reconstructions are succeeded by halting the ML algorithm reasonably early in the optimization process.

A rationalization for implementing a stopping criterion needs some further insight. When a stopping criterion is employed, the initial estimate acts a noteworthy part in the reconstruction. To evaluate this role, we proceeds a handier expression at the iterative reconstruction process. Iterative reconstruction algorithms are typically primed by way of a uniform, constant estimate. An algorithm then iterates towards the solution in steps of varying size and direction. Given the data and the initial estimate, the path is specified by the particular choice of optimization algorithm.

Such a process for a MLEM algorithm is represented in Fig. 2 where the dotted contours represent contours of constant likelihood. In halting the algorithm prematurely, one accepts some estimate along the optimization path, as at the point marked as colored in Fig. 2.

Starting from a constant initial estimate, the reconstruction of a source from mechanically collimated data retains some of the smoothness of that initial estimate for a number of iterations of a MLEM algorithm. After some 30 iterations of the MLEM algorithm the reconstruction becomes excessively non smooth.

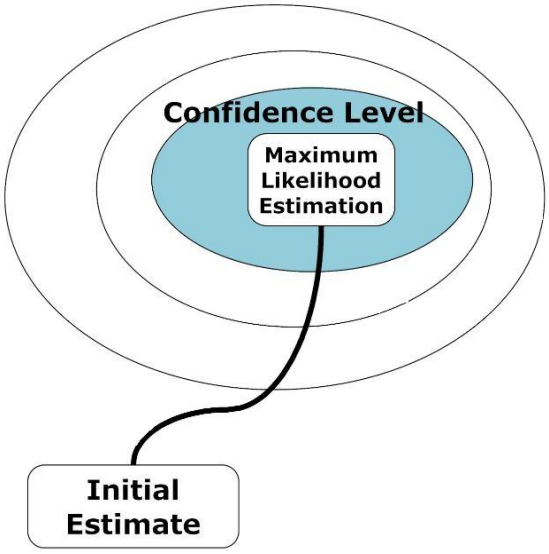

Fig. 2: An Iterative optimization Process

Starting from a constant initial estimate λ_c, it is apparent that an iterative MLEM reconstruction retains some of the smoothness of that initial estimate during the initial iterations. The effect of the constant initial estimate has been to anchor the free end of the optimization path (the initial point) such that the path passes through smoother estimates than those

traversed when the procedure is primed by means of a pseudo-random estimation. One would therefore like some strategy of effecting a trade-off between the smoothness of the constant initial estimate λ_c and the asymptotic consistency and efficiency of the ML estimate λ_{ML}, such an approach provides a justification and the method for applying smoothed versions of iterative algorithms.

A trade-off between λ_c and λ_{ML} is mostly aptly defined by a confidence region. The determination of a stopping point can be posed as a hypothesis test. Statistics for which this test performs well for sources within a wide range of complexity are sought. The performances of these statistics are compared.

In using a hypothesis test as a stopping criteria, the null hypothesis is that the data y are Poisson with vector of parameters $(p\hat{\lambda}^k)$ where $\hat{\lambda}^k$ is the estimate at the K^{th} iteration. A test statistics s_t having a known density function under a correct null hypothesis is formulated. A critical region, consisting of all values outside some confidence interval $[a, b]$, and a significance level α are choosen such that if the null hypothesis is correct $p(a < S_i < b) = 1 - \alpha$. The hypothesis is tested by computing the statisticss_i, a function of λ^k and y. If $s_t < a$ or $s_t > b$ the null hypothesis is rejected at the α importance glassy and an alternate estimate of λ is sought. Otherwise, the estimate $\hat{\lambda}^k$ is accepted and the algorithm terminated.

ML-EM may require from 10-100 iterations depending on the stopping rule used. Several methods have been suggested to decrease the calculation time in the ML-EM algorithm. The most common tactic exist is OS-EM method proposed by Hudson and Larkin in 1994. In this method, forecast statistics is separated keen on subsets and uses solitary one subset for each iteration. OS-EM has evidenced en route for the rebuilding maximized time on behalf of the reconstruction by a factor of 6.

System Design and Implementation

Data Set

To implement MLEM Shepp-Logan phantom image of various sizes such as 64 x 64, 128 x 128 and 256 x 256 is taken for study to reconstruct an image. The radon function present in Matlab is utilised to retrieve projection data of the sampled image rotated on a specified angles. This system uses five different angles, such as 6^0, 9^0, 12^0, 15^0, 18^0 obtaining 30, 20, 15, 12, 10 numbers of projections respectively The projection of a two dimensional function $f(x, y)$ is a set of line integrals. The $f(x, y)$ is transferred to a column vector. The photons emitted p_i passed at a specified angle collects data by calculating the weight matrix. Using these data as input MLEM algorithm reconstruct an image both sequentially and in parallel version.

Sequential version

MLEM implemented in the single core is depicted as sequential version. With the projection data obtained and the Initial guess of the estimate MLEM algorithm is passed as input to reconstruct an image. MLEM is an iterative reconstruction method based on statistical data, the required iteration has been optimized based on the PSNR value. This is followed by calling a MEX function consisting of MLEM algorithm in a single core. The time taken to reconstruct an image is noted for each size at different angles of projections.

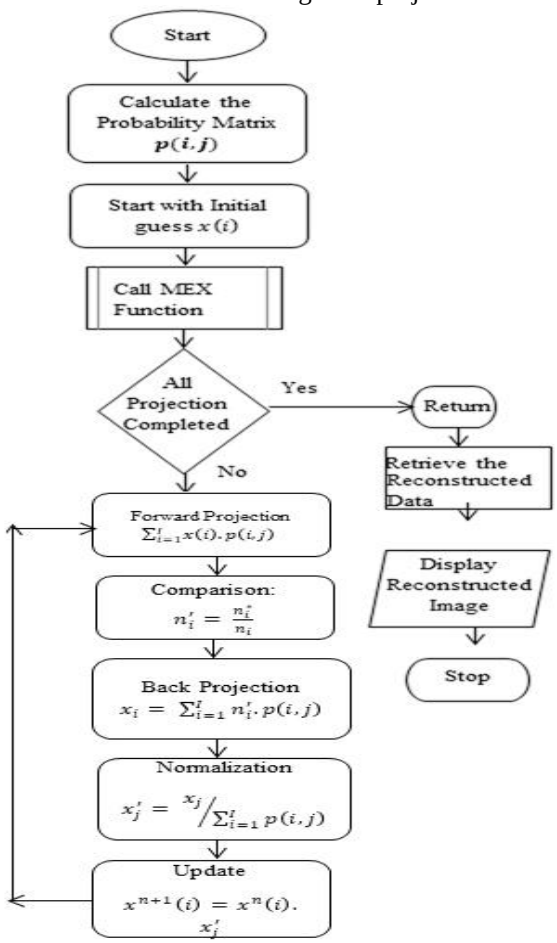

Fig. 3 (a): Flowchart of MLEM to reconstruct an image in sequential mode

Fig. 3 (a) gives the pictorial representation for the steps involved in reconstructing an image using MLEM. As described in the methodology first forward projection followed by comparison, Back projections, normalization and value updating for all numbers of projection data.

Parallel Version

The iterative statistical pMLEM algorithm is implemented under the multi-core is considered as parallel version. Similar steps exist as in sequential version. Optimizing the iterations are carried out in Matlab and image reconstruction algorithm MLEM for calculating the each pixel value for each projection is done in parallel by calling the MEX function. In the MEX function the number of cores are set to 2, 4 or 8 using the OMP_SET_NUM_THREAD(num_thread) function. Initially the program starts with single core. #pragma omp parallel directive is used to create a master and a worker thread. The Master thread co-distributes the measured and the calculated projection data to the worker thread. After updating the value each worker updates its value and the master thread update the final value in the vector. Fig. 3 (b) is the flow chart representing the parallel version of MLEM.

Implementation

Sequential version

The pseudo code of MLEM algorithm executed using single core is given in Table 4.1. The steps described in the design section have been implemented in this algorithm. The calculation part of Forward projection, back projection, normalization and value updating is done using single core. To select a single core OMP_NUM_THREADS(num_thread) is passed with value 1.

Table 4.1: ML-EM Algorithm

```
mlem(){
    if not reached all projections()   {
        for all elements in the projection {
            Calculate forward projection;
            Compare the measured and calculated data;
            Calculate the back projection and perform
normalization;
            Update the value;
        }
    }
}
```

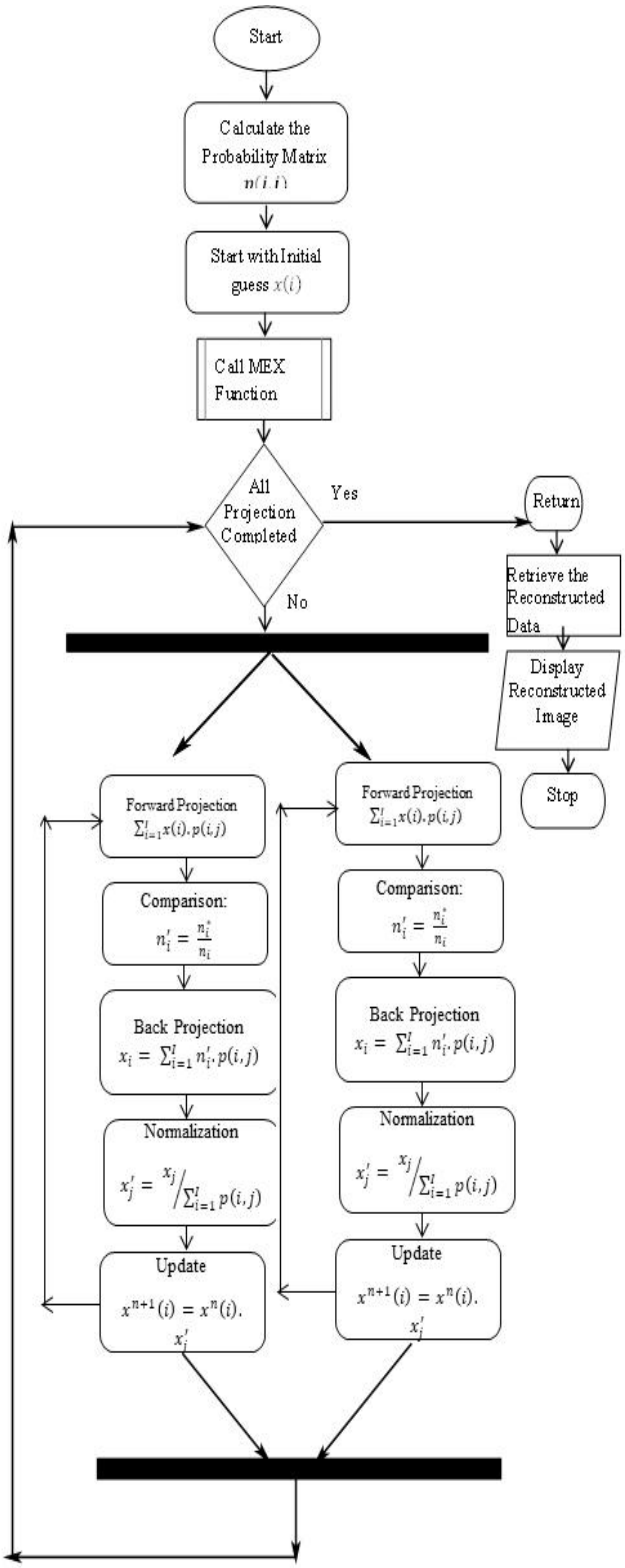

Fig. 3 (b): Flowchart of MLEM to reconstruct an image in parallel mode

Parallel version

Table 4.2 tabulate the pseudo code of the proposed pMLEM algorithm to reconstruct the Shepp-Logan Phantom in 2, 4 and 8 cores in order to decrease the time complexity the MLEM algorithm suffers. The time complexity reduction is proved in the results and discussion section.

Table 4.2 Proposed pMLEM algorithm

```
pmlem(){
   If not reached all projections(){
omp_set_num_threads(number_of_threads);
        #pragma omp parallel for shared(elements)
private(index) schedule

(dynamic, num_elements)
       For all elements in the projection{

omp_set_num_threads(number_of_threads);
         #pragma omp parallel for shared(elements)
private(index)
                  schedule(dynamic, num_elements)
reduction(+:calculated value)
           Calculate forward projection;
           Compare the measured and calculated
data;
           Calculate the back projection and perform
normalization;
           Update the value;
       }
   }
  Recursively call pmlem function for remaining
projections
}
```

Results and Discussion

Statistical Image reconstruction algorithm MLEM is evaluated. MLEM is also an iterative based algorithm. It is compared with standard algorithms like FBP, SIRT, SART and ART which motivated to parallelize MLEM algorithm in a multicore environment.

The performance exploration of this technique on behalf of image reconstruction is analysed in this chapter.

SIRT, SART, ART and MLEM algorithms are input with projection matrix, weighted matrix and number of iterations. The projections matrix and the weight matrix sizes are already discussed in chapter 3 results and discussion section.SIRT, SART and MLEM uses the iteration optimised using MLEM algorithm and for ART the iteration optimised in chapter 3 is used. The optimized iteration is shown in the Table 4.3.

The parameters used to reconstruct the image are projections matrix, Weight matrix and iterative algorithms such as SIRT, SART, ART, MLEM and pMLEM in preferred angle such as 18^0 producing 10 numbers of projections, 15^0 yielding 12 numbers of projections, 12^0 producing 15 numbers of projections, 9^0 producing 20 numbers of projections and 6^0 producing 30 number of projection is considered for study. **To** reconstruct 128 x 128 image size various parameters of projection matrix at angles as mentioned in chapter 3 and the weight vector as a sparse matrix in size 16384 x 1 and number of optimised iteration required are the elementary input passed in the specified algorithm.SIRT, SART, MLEM and pMLEM is measured for the optimised number of iterations using MLEM algorithm. The FBP algorithm is a non-iterative algorithm. It does not hold the number of iterations. The FBP measured in Chapter 3 for various angle is considered throughout the study.

With the projections matrix with 367 x number of projections and 65536 x 1 vector a 256 x 256 image reconstructed using FBP, SIRT, SART, MLEM and pMLEM is shown in Fig. 4.12. The number of iterations required to acquire a free artifact images is tabulated in Table 4.9.PSNR value obtained for reconstructing 256 x 256 image is tabulated in Table 4.10 and graphed in Fig. 4.13. Similarly time taken to reconstruct the same image withthe same number of iterations as listed above is given in Table 4.11 and Fig. 4.14. pictures the relevant data.

Number of iterations

Table 4.11 shows the number of iterations optimized to reconstruct the Shepp-Logan phantom images using MLEM for various sizes such as 64 x 64, 128 x 128 and 256 x 256 at different projection angles 30, 20, 15, 12, 10 is tabulated and their responses are plotted in Fig. 4.15.

The tabulation shows the number of iterations increases only on the size of images not on the basis of number of projections as ART algorithm performed.

Table 4.9. Optimized iteration to reconstruct 256 x 256 images with high perceptual fidelity using SIRT, SART, ASRT, MLEM and pMLEM

Algorithms	**Number of projections**				
	10	**12**	**15**	**20**	**30**
SIRT, SART, MLEM and pMLEM	59	40	51	40	69
ART	158	142	124	46	24

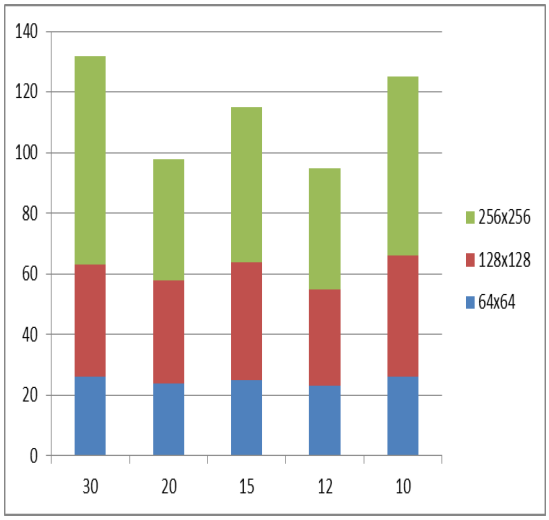

Fig. 4.15. Graph showing the optimised number of iterations required to reconstruct the images.

Peak Signal-to-Noise Ratio

Table 4.12 shows the analysis of PSNR value for reconstructing the images in single core and multi core environment. In this table, the PSNR value can be analysed for different image sizes with various number of projections. It is observed that the PSNR for different size of images using various angles is above 60 db which shows the tremendous perceptual fidelity.

The PSNR values that are obtained for various image sizes at different angles are plotted in Fig. 4.15. It is necessary to highlight that the PSNR values obtained for the reconstructed image sequentially and parallel has the same value. This depicts that the parallel programming maintains the image quality as it is.

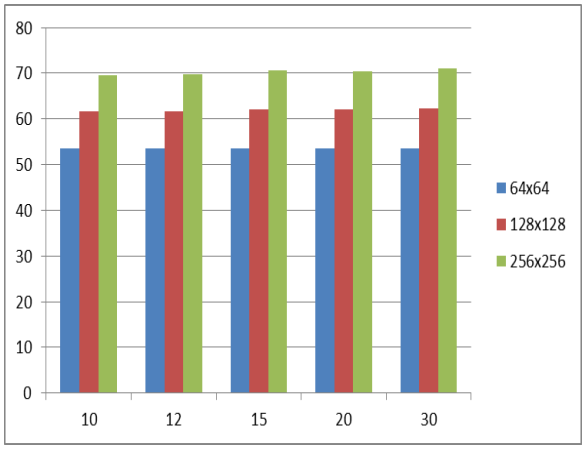

Fig. 4.15. Plotted the PSNR value obtained while reconstructing Shepp Logan Phantom Images on 64x64, 128x128 and 256x256 sizes using 30, 20, 15, 12 and 10 numbers of projections in sequential and parallel version

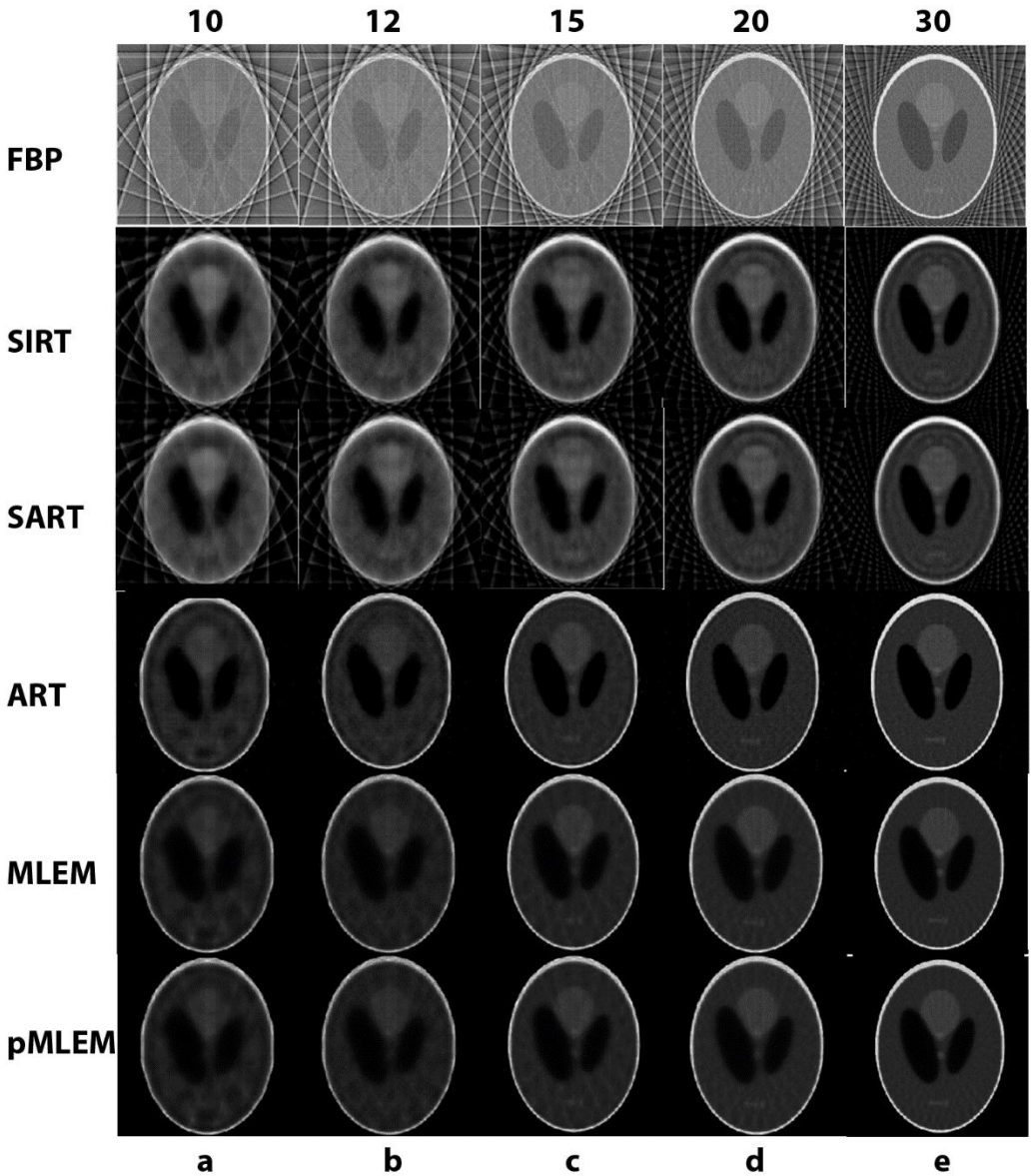

Fig. 4.12. 256 x 256 Shepp Logan phantom reconstructed using FBP, SIRT, SART, ART, MLEM and pMLEM using (a) 10, (b) 12, (c) 15, (d) 20, (e) 30 numbers of projections obtained at 18^0, 15^0, 12^0, 9^0 and 6^0.

Table 4.10. Tabulated the PSNR value measured for the 256 x 256 image reconstructed with projection data obtained at 18^0 degree with 10 number of projections, 15^0 degree with 12 number of projections, 12^0 degree with 15 number of projections, 9^0 degree with 20 number of projections and 6^0 degree with 30 number of projections.

	10	12	15	20	30
FBP	58.0899	59.0863	60.4143	62.0325	64.4252
SIRT	65.3219	65.6799	66.364	67.1133	68.583
SART	65.3502	65.7131	66.4068	67.2005	68.648
ART	69.3787	69.5936	70.676	70.3131	71.0605
MLEM	69.5807	69.7042	70.5335	70.4742	71.0236
pMLEM	69.5807	69.7042	70.5335	70.4742	71.0236

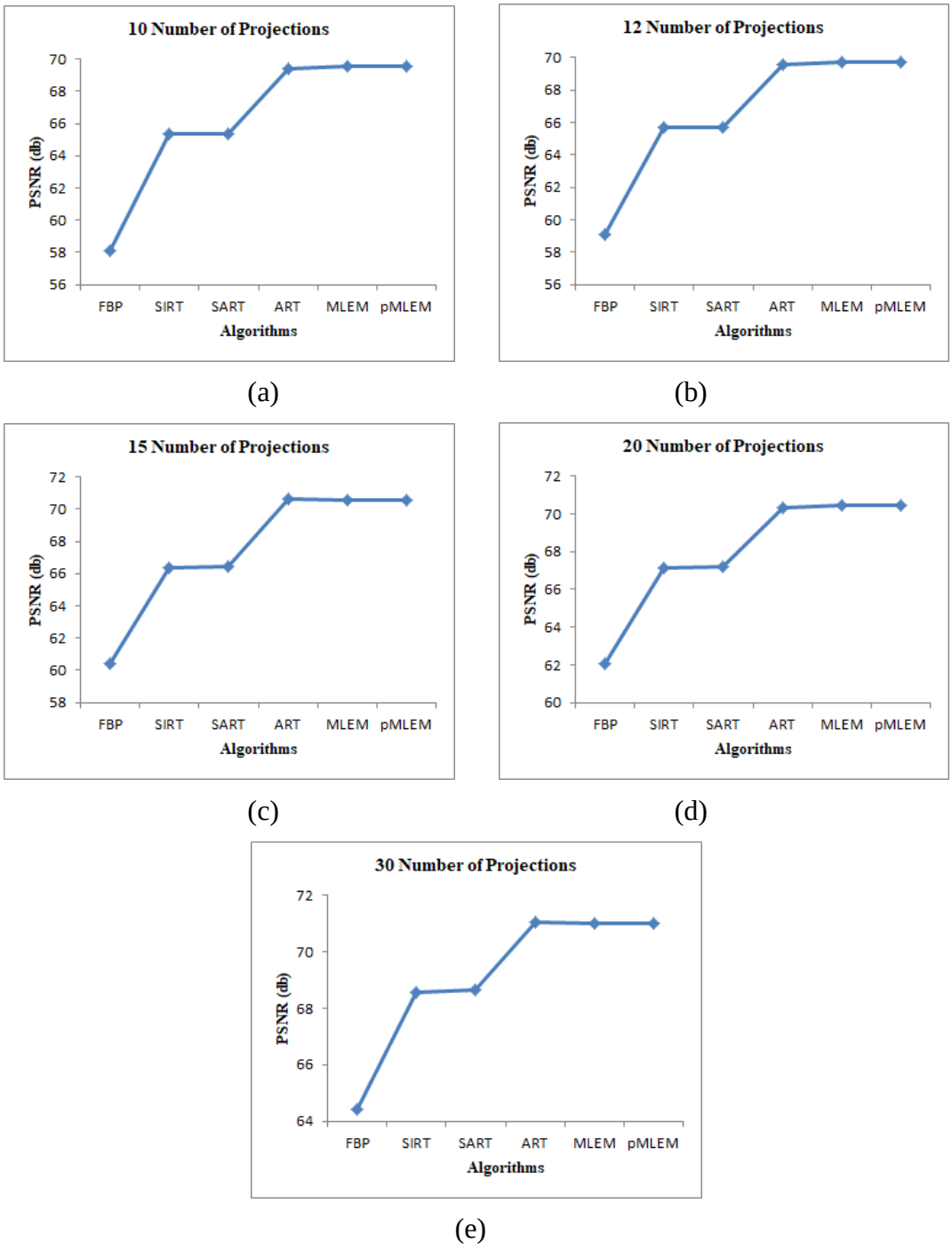

Fig. 4.13. A Graph showing the time consumed to reconstruct 256 x 256 image using FBP, SIRT, SART, ART, MLEM and pMLEM with (a) 10, (b) 12, (c) 15, (d) 20, (e) 30 number of projections.

Table 4.11. Time taken by FBP,SIRT, SART, ART, MLEM and pMLEM to reconstruct 256 x 256 image using various number of projections.

	10	12	15	20	30
FBP	0.008455	0.007704	0.00781	0.015839	0.021083

SIRT	81.4186	73.2486	117.1321	83.1238	214.6706
SART	65.1944	58.721	79.3762	65.7881	198.9407
ART	1609.1	1699.73	1889.8	918.3131	723.983
MMLEM	522.894	462.973	750.215	709.861	2134.4
2Core	508.943	341.971	743.438	766.535	1987.55
4Core	375.436	266.157	435.619	550.758	1304.25
8Core	200.919	179.447	264.467	485.687	797.848

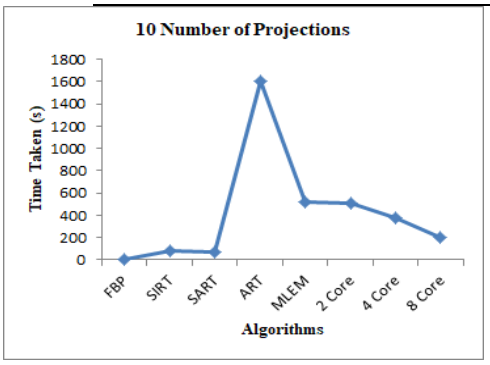

(a)

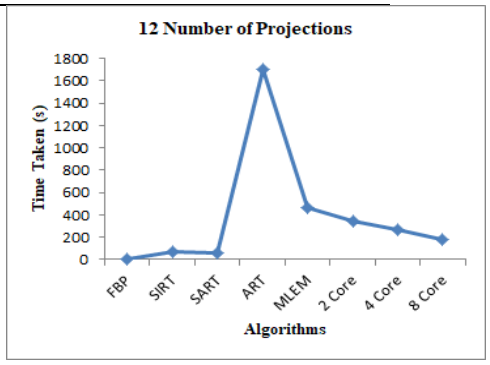

(b)

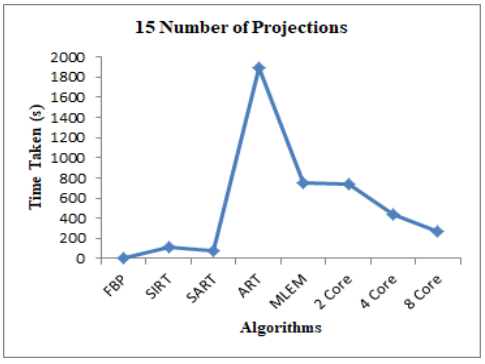

(c)

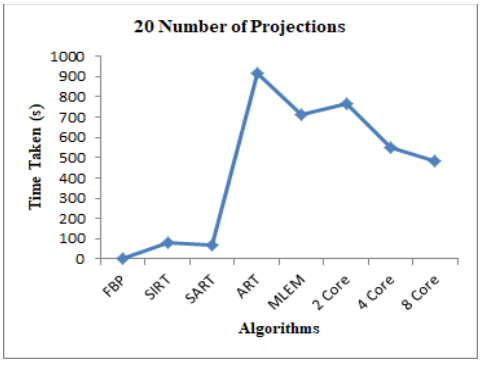

(d)

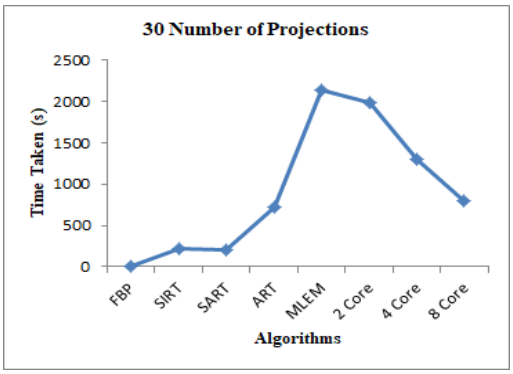

(e)

Fig. 4.14. Time achieved to reconstruct 256 x 256 image with projections data obtained at (a) 18^0, (b) 15^0, (c) 12^0, (d) 9^0, (e) 6^0 using FBP, SIRT, SART, ART, MLEM and pMLEM using 2, 4 and 8 cores.

During the study using above diagrammed data the image quality throughout the various size considered for study shows more or less same or slightly improved quality. But the quality of the image has not gone through in reverse. Image size 128 x 128 time taken to reconstruct strategy shows a prominent difference between ART and MLEM even for minimum number of projections data. This stimulates

the entire study to implement the algorithm in shared memory environment to reduce the time further.

Performance measures

The metric used to validate the reconstructed image are PSNR value of an image, time taken to reconstruct an image and the speed up using Amdhal's law to analyse the system's performance.

Time complexity

Time complexity is measured using the tic and toc command in MATLAB. The time taken to reconstruct an image using MLEM and pMLEM in sequential using 1 core and parallel using 2, 4 and 8 cores in AMD processor respectively is charted in Table 4.13, 4.14 and 4.15 for 64 x 64, 128 x 128 and 256 x 256 image size respectively.

The time complexity indicates the degree of user utility. As a result, for limited number of projections it takes high time complexity in single core execution. But, for each number of projections for all sizes of images the time complexity has been reduced. Fig. 4.18, Fig. 4.19, Fig. 4.20 shows the performance of the parallel system. The reduction in time complexity indicates the high degree of user utility. This proves that parallel programming can be used as tool to reduce the time of execution.

Speed up

The analysis of speedup calculation for MLEM is obtained by applying the Amdahl's law for the serial and parallel time. Table 4.16, 4.17 and 4.18 shows the speedup calculation for the image of sizes 64 x 64, 128 x 128 and 256 x 256 respectively. Also this speedup calculation is plotted against the different reconstructed image sizes at various projection angles and different number cores 1, 2, 4 and 8.

Table 4.15. Time complexity for 256 x 256 phantom reconstructed image size

Cores	Number of projections				
	10	12	15	20	30
1	522.894	462.973	750.215	709.861	2134.4
2	508.943	341.971	743.438	766.535	1987.553
4	375.436	266.157	435.619	550.758	1304.245
8	200.919	179.447	264.467	485.687	797.848

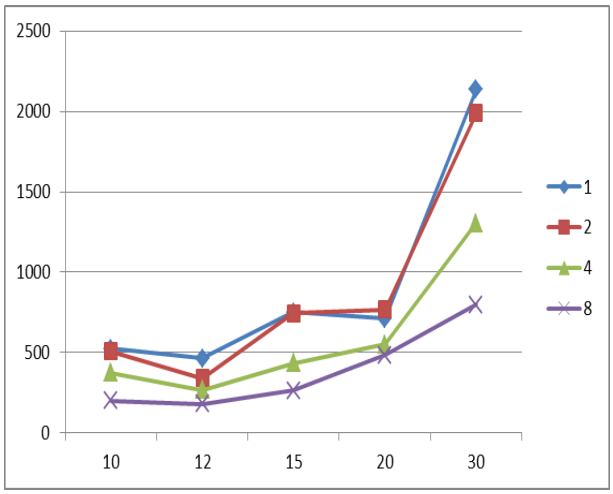

Fig. 4.18 A graph showing the Time Complexity of reconstructing Phantom image of size 256 x 256 sequentially, parallel in 2, 4 and 8 core with respect to projections.

The performance analysis of MLEM for reconstructed image size of 64 x 64, 128 x 128 and 256 x 256 with varying projection angles is tabulated in table 4.16, 4.17 and 4.18 respectively. The graph plotted in Fig. 4.19 shows that the performance gradually increasing as the number of cores increases. The evaluation results depicts that the MLEM architecture

for 64 x 64 image size performs faster under different number of cores.

Similarly for 128 x 128 and 256 x 256 image size speed up is plotted in Fig. 4.20 and Fig. 4.21. Both The graph shows that the performance gradually increases with increase in the number of cores.

Table 4.18. Speedup calculation for 256 x 256 size reconstructed phantom image

cores	Number of projections				
	10	12	15	20	30
1	1	1	1	1	1
2	1.207948	1.739887	1.704303	1.636929	1.617992
4	1.218398	2.386777	2.260526	2.168257	2.176752
8	1.245951	3.143542	3.084992	3.154823	2.893623

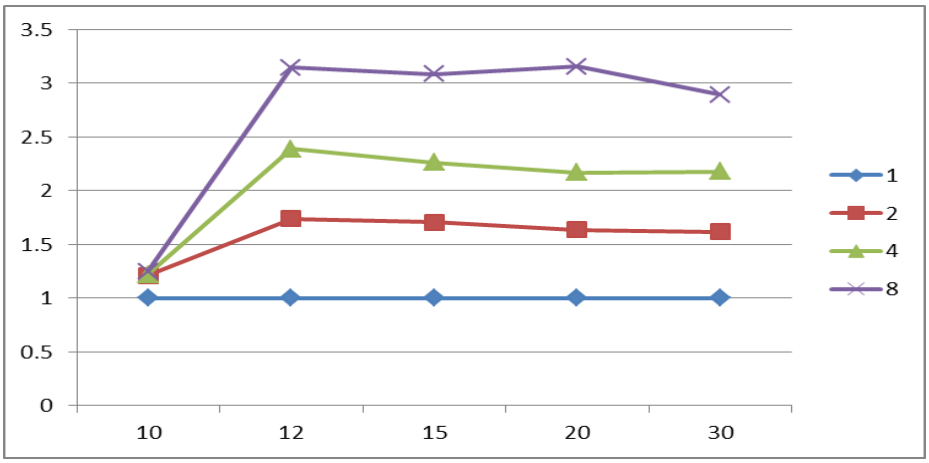

Fig. 4.21: A graph showing the Performance Analysis of the multi-core environment for the image reconstructed for 256 x 256 at varying number of projections under 1, 2, 4 and 8 cores

From the Results so for discussed proves that the size and the number of projection does not affects the parallel programming. The higher the data size yields the better performance while using parallel programming.

Summary

Medical Image process affords a non-invasive practice to learn at the basic and purposeful statistics of internal organs and structures. Measuring the radioactive distribution all the way through the patient offers the physiological and patho-physiological evidence related to the patient. The most widely used mathematical technique to reconstruct this image, using the data assimilated, is recognized as Filtered Back Projection (FBP). The foremost perseverance of this research work is to substantiate whether or not we can rebuild artefact free images with limited dataset instantaneously.

An attempt is made using ML-EM, by enhancing the probability matrix (system matrix) with simple substitutions. Diagonal elements related to the system matrix are given through the corresponding projection data elements. Therefore, to remove the detectors from the reconstruction procedure, we can replace the value by the average assessment of the diagonal matrix. The Enhanced ML-EM algorithm is a good alternative to the filtered back projection algorithm and can be used successfully to reconstruct artefact free images with limited dataset. All the reconstruction done in our study was done using Matlab. The results have shown reconstructing an image quickly as number of cores increases. It also proven that parallel programming has high efficiency using Amdhal's law.

References

[1] Scholl, T. Aach, T. M. Deserno, and T. Kuhlen, "Challenges of medical image processing," Computer science-Research and development, vol. 26, pp. 5-13, 2011.

[2] R.Murugesan, M.Afeworki, J.A.Cook, N.Devasahayam, R.Tschudin, J.B.Mitchell, S.Subramanian, and M.C.Krishna. A broadband pulsed radio frequency electron paramagnetic resonance spectrometer for biological applications. Review of Scientific Instruments, 69(4), April 1998.

[3] G.L.Zeng. Image reconstruction a tutorial. Computerized Medical Imaging and Graphics, 25, 2001.

[4] P.F.C.Gilbert. Iterative Methods for the three dimensional reconstruction of an object from projections. Journal of Theory, Biology, 36, July 1972.

[5] P.M.V.Subbarao, P.Munshi, and K.Muralidhar. Performance of iterative tomographic algorithms applied to non destructive evaluation with limited data. NDT and E International, 30, 1997.

[6] J. Treibig, G. Hager, H. G. Hofmann, J. Hornegger, and G. Wellein, "Pushing the limits for medical image reconstruction on recent standard multicore processors," The International Journal of High Performance Computing Applications, vol. 27, pp. 162-177, 2013.

[7] S.Sivakumar, MuraliC.Krishna, R.Murugesan. Evaluation of Algebraic Iterative Algoritms for Reconstruction of Electron Magnetic Resonance Images, September 2010.

[8] C.N.Smith and A.D.Stevens. Reconstruction of images from radiofrequency electron paramagnetic resonance spectra. The British Journal of Radiology, 67, 1994.

[9] M. Beister, D. Kolditz, and W. A. Kalender, "Iterative reconstruction methods in X-ray CT," PhysicaMedica: European Journal of Medical Physics, vol. 28, pp. 94-108, 2012.

[10] G. Wang and J. Qi, "PET image reconstruction using kernel method," IEEE transactions on medical imaging, vol. 34, pp. 61-71, 2015.

[11] M. M. Khalil, J. L. Tremoleda, T. B. Bayomy, and W. Gsell, "Molecular SPECT imaging: an overview," International journal of molecular imaging, vol. 2011, 2011.